Available online at www.sciencedirect.com
ScienceDirect
Journal of Sound and Vibration 306 (2007) 349–360
JOURNAL OF SOUND AND VIBRATION
www.elsevier.com/locate/jsvi

Short Communication

Damping cable vibration for a cable-stayed bridge using adjustable fluid dampers

Y.L. Xu*, H.J. Zhou

Department of Civil and Structural Engineering, The Hong Kong Polytechnic University, Hung Hom, Kowloon, Hong Kong

Received 2 February 2007; received in revised form 16 May 2007; accepted 19 May 2007
Available online 2 July 2007

Abstract

Passive fluid damper is one of most widely used control devices for damping vibration of stay cables in a cable-stayed bridge in practice. However, each stay cable features unique dynamic characteristics and requires a specific damper to achieve the best control performance, which engenders many troubles in manufacture, implementation and maintenance of dampers. This paper presents a new approach for damping vibration of stay cables in a cable-stayed bridge by using adjustable fluid dampers. The principle and main features of adjustable fluid dampers with shape memory alloy (SMA) actuators are first introduced. The solution of a taut cable with the adjustable fluid damper described by the Maxwell model is provided. A most favorable design principle is then proposed for selecting the least types of adjustable fluid dampers for damping vibration of a few hundreds stay cables in a cable-stayed bridge. A case study of stay cables in a super long span cable-stayed bridge is finally performed, demonstrating that only two types of adjustable fluid dampers are required for damping vibration of all stay cables in the bridge.

1. Introduction

Stay cables in a cable-stayed bridge have frequently exhibited large-amplitude vibrations under wind, wind-rain or parametric excitations [1–3]. Though the mechanisms of some excitations have not been well understood yet, practical measures have been taken to prevent cable vibrations, in which passive fluid damper is one of most widely used control devices installed near cable anchorage for damping cable vibration. Theoretical studies were also carried out to evaluate the increased damping level of a stay cable after installing passive fluid dampers and to facilitate the design of passive fluid dampers [4–9]. It was found that there exists an optimum viscous coefficient of the damper by which the modal damping ratio of a stay cable can reach its maximum for a given mode of vibration. However, if the viscous coefficient of the damper deviates from its optimum value, the modal damping ratio of the stay cable decreases rapidly. As each stay cable in a cable-stayed bridge features unique dynamic characteristics, a specific fluid damper is required to achieve the best vibration mitigation for a given mode of vibration. This requirement engenders many troubles in manufacture, implementation and maintenance of fluid dampers for a cable-stayed bridge. The use of magnetorheological

*Corresponding author. Tel.: +852 27666050; fax: +852 23346389.
E-mail addresses: ceylxu@polyu.edu.hk (Y.L. Xu), cehzhou@polyu.edu.hk (H.J. Zhou).

0022-460X/$ - see front matter © 2007 Elsevier Ltd. All rights reserved.
doi:10.1016/j.jsv.2007.05.032

(MR) dampers with semi-active control algorithm [10] may be an alternative but some practical issues need to be solved before it can be accepted by engineering professions.

To overcome this problem, an adjustable fluid damper with shape memory alloy (SMA) actuators has been recently developed by Li et al. [11]. Instead of the fixed number of orifices in the piston head of a common fluid damper, SMA actuators are installed inside the piston head to control the number of orifices so as to change damper parameters for the best control of a group of stay cables. After the optimum viscous coefficient of the damper of an adjustable fluid damper is achieved for a given cable, the damper then works as a passive damper to maintain the practical merit of passive fluid dampers. The adjustable fluid damper was designed and manufactured. The performance tests of the damper were carried out within a range of frequencies and amplitudes and for a number of open orifices and two sizes of orifices. The test results [11] showed the mechanical behavior of damper could well be described by the Maxwell model. However, in most of the previous studies the passive fluid damper is assumed as a classical linear dashpot in which the damper force is directly proportional to the piston velocity for mathematical simplicity of analyses. This assumption may overestimate the damping ratio of a stay cable provided by a fluid damper [7]. Therefore, the incorporation of the Maxwell model for a fluid damper into the cable–damper system is necessary, which not only reflects the displacement dependent behavior of a fluid damper but also enables one to consider the effect of damper support stiffness if necessary.

This paper presents a new approach for damping vibration of stay cables in a cable-stayed bridge by using adjustable fluid dampers. The principle and main features of adjustable fluid dampers with SMA actuators are first introduced. The solution of a taut cable with the adjustable fluid damper described by the Maxwell model is provided based on the work of Krenk [5] and Main and Jones [6]. A most favorable design is then proposed for selecting the least types of adjustable fluid dampers for damping vibration of a few hundreds stay cables in a cable-stayed bridge. A case study of stay cables in a super long span cable-stayed bridge is finally performed in this paper.

2. Adjustable fluid damper with SMA actuators

Different from a common passive fluid damper with a fixed number of orifices in its piston head, SMA actuators are installed inside the piston head in an adjustable fluid damper to control the number of orifices so as to change damper parameters for the best control of a group of stay cables. After the optimum viscous coefficient of the damper of an adjustable fluid damper is achieved for a given cable, the damper then works as a passive fluid damper to maintain the practical merit of passive fluid dampers. A SMA actuator possesses at least two main characteristics: (1) it could control a small mechanical valve inside the damper piston to close or open an orifice; and (2) the mechanical valve could be firmly locked at a prescribed position within a working temperature range. A schematic diagram of a SMA actuator is shown in Fig. 1(a), and the SMA actuators installed in the piston of a prototype adjustable fluid damper are depicted in Fig. 1(b). There are two SMA wires, each of which is connected to one end of the valve block and fixed on the piston via two pulleys. By using an impulse current to heat one wire each time, the SMA wire will pulls the valve block to open or close an orifice through the positioning plate and locating ball. Two types of prototype adjustable fluid dampers were designed and manufactured: type 1 with 1.5 mm diameter orifices for large viscous coefficient of the damper; and type 2 with 1.8 mm diameter orifices for relatively small viscous coefficient of the damper. The two prototype dampers were extensively calibrated and tested, and the experimental results demonstrated that the damper performance could be well described by the following Maxwell model (e.g. Ref. 12):

$$F_d + \lambda_d \frac{\mathrm{d}F_d}{\mathrm{d}t} = c_d v \tag{1}$$

in which F_d is the damper force; λ_d is the relaxation time constant; c_d is the viscous coefficient of the damper at zero frequency; and v is the velocity of piston head. Table 1 lists the experiment results of the viscous coefficient of the dampers and relaxation time constants of the two types of adjustable fluid dampers developed. It can be seen that the relaxation time constant increases with increasing viscous coefficient of the damper at zero frequency. Both the viscous coefficient of the damper at zero frequency and the relaxation time

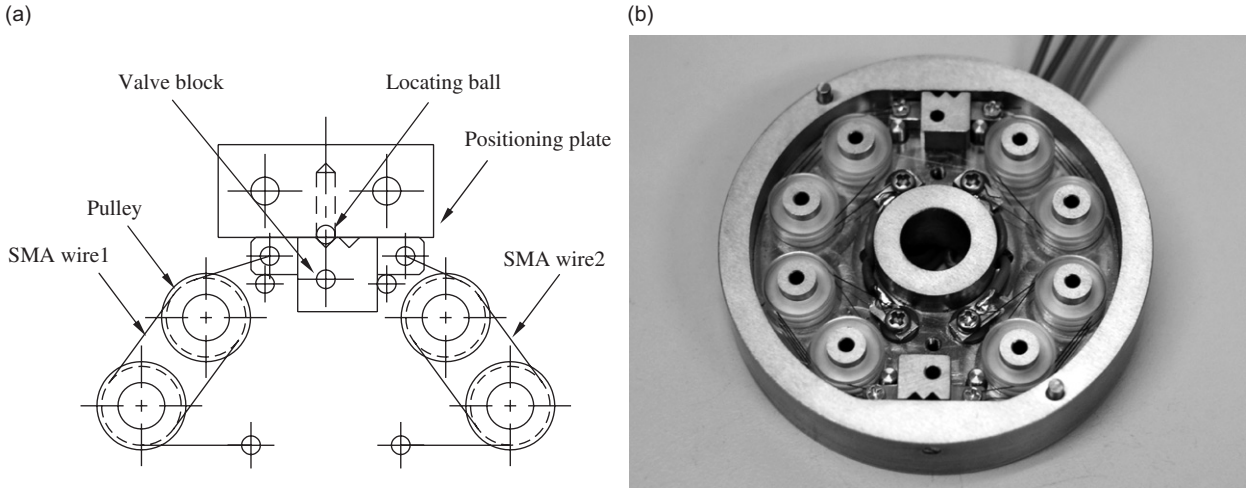

Fig. 1. Principle and prototype of SMA actuator: (a) schematic diagram of SMA actuator and (b) prototype of SMA actuator within a piston.

Table 1
The viscous coefficient of the dampers c_d and relaxation time constants λ_d of two types of adjustable fluid dampers against the opened orifice number n

n	Damper type 1 (1.5 mm orifices)		Damper type 2 (1.8 mm orifices)	
	c_d (N s/m)	λ_d (s)	c_d (N s/m)	λ_d (s)
10	137 000	0.0038	89 000	0
9	149 000	0.0053	101 000	0
8	173 000	0.0059	112 000	0.0013
7	198 000	0.0066	129 000	0.0021
6	228 000	0.0102	146 000	0.0056
5	267 000	0.0128	169 000	0.0069
4	332 000	0.0164	213 000	0.0098
3	446 000	0.0212	278 000	0.0158
2	621 000	0.0338	427 000	0.0228

constant become larger as the opened orifice number n becomes smaller. More details on adjustable fluid dampers and the test results could be found in Li et al. [11].

3. Approximate solutions of cable–damper system

In consideration that most stay cables in a cable-stayed bridge are of small sag in the order of 1% sag-to-length ratio but with a high tension-to-weight ratio [3], only a taut cable with an adjustable fluid damper installed near one of cable anchorage is considered, as shown in Fig. 2. The adjustable fluid damper described by the Maxwell model can be represented by a dashpot and a spring connected in series. The effect of the damper support is also considered in terms of a spring connected to the damper in series. If the length between the left cable anchorage and the damper is denoted as l_1, the length between the right cable anchorage and the damper is $l_2 = L - l_1$, in which L is the total length of the cable. In practice, the length l_1 is much smaller than the length l_2. The internal structural damping of a stay cable is very small compared with the damping provided by a properly designed fluid damper and it is thus neglected in this study. By considering the cable–damper system in two parts x_1 and x_2 using the damper position as a division, the free vibration of the cable–damper system in the transverse direction can be described by the following partial differential equation

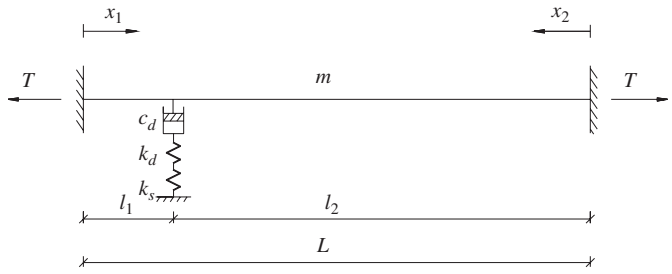

Fig. 2. A taut cable with a fluid damper near its anchorage.

for each part of the cable:

$$m\frac{\partial^2 w_k(x_k,t)}{\partial t^2} = T\frac{\partial^2 w_k(x_k,t)}{\partial x_k^2} \quad (k=1,2) \tag{2}$$

in which $w_k(x_k, t)$ is the transverse displacement of the cable at point x_k, and x_k is the coordinate along the cable chord axis in the kth part; m is the cable mass per unit length; and T is the cable tension force. The boundary conditions of the two parts of the cable are $w_1(0, t) = w_2(0, t) = 0$ for all t.

At the damper location, there is a discontinuity in cable slope, providing a transverse force matching the damper force F_d.

$$T\left[-\frac{\partial w_2}{\partial x_2}\bigg|_{x_2=l_2} - \frac{\partial w_1}{\partial x_1}\bigg|_{x_1=l_1}\right] = F_d. \tag{3}$$

Since the velocity of the damper piston is the same as the velocity of the cable at damper location, Eq. (1) could be rewritten as

$$F_d + \lambda\frac{\mathrm{d}F_d}{\mathrm{d}t} = c_d\frac{\partial w_1}{\partial t}\bigg|_{x_1=l_1}, \tag{4}$$

where

$$\lambda = \lambda_d + \lambda_s = c_d/k_d + c_d/k_s \tag{5}$$

in which λ is the total relaxation time constant considering both damper stiffness and damper support stiffness; λ_d is the relaxation time constant of damper itself; λ_s is the equivalent relaxation time constant of damper support; k_d is the damper stiffness; and k_s is the damper support stiffness.

Although the Maxwell damper was not considered by Main and Jones [6] and Krenk and Høgsberg [7], the frequency equation of the cable with an adjustable fluid damper can be obtained by simply substituting the complex mechanical impedance $c_d/(1+\lambda\omega_{o1}\chi)$ in place of the viscous coefficient c in Eq. (6) of the literature [6].

$$(1+\lambda\omega_{o1}\chi)\left[\coth\left(\pi\chi l_1/L\right)+\coth\left(\pi\chi l_2/L\right)\right]+\frac{c_d}{\sqrt{Tm}}=0, \tag{6}$$

where χ is the dimensionless eigenvalue that is complex in general; and $\omega_{o1} = (\pi/L)\sqrt{T/m}$ is the first circular natural frequency of the taut cable without damper.

For specific values of $c_d/\sqrt{Tm}$, l_1/L and $\lambda\omega_{o1}$, Eq. (6) can be directly solved numerically to obtain a series of complex eigenvalues. In practice, the damper is often installed near the cable anchorage and l_1/L is rather small. Cable vibration mitigation also focuses on the first few modes of vibration only. Based on Eq. (6) and the work of Main and Jones [6], the approximate (asymptotic) solution of the ith nondimensional modal damping ratio of the cable–damper system can be found as

$$\frac{\zeta_i}{l_1/L} \cong \frac{\pi^2\kappa_i}{1+(\pi^2\kappa_i+\mathrm{i}\lambda\omega_{o1})^2}, \tag{7}$$

where

$$\kappa_i \equiv \frac{c_d}{mL\omega_{o1}} i(l_1/L) \tag{8}$$

in which κ_i is termed the nondimensional viscous coefficient of the damper for the ith mode of vibration. It can also be found from Eq. (7) that the maximum attainable damping ratio is $\zeta_{i,\max} \cong \frac{1}{2}\frac{l_1}{L}\left[\sqrt{(i\lambda\omega_{o1})^2+1} - i\lambda\omega_{o1}\right]$ when $\kappa_{i,\text{opt}} = \sqrt{1+(i\lambda\omega_{o1})^2}/\pi^2$, where $\kappa_{i,\ \text{opt}}$ is the optimal nondimensional viscous coefficient of the damper to achieve the maximum attainable modal damping ratio $\zeta_{i,\ \max}$.

Fig. 3(a) displays the asymptotic solutions for $\zeta_i/l_1/L$ and κ_i for the first five modes of vibration, obtained using Eq. (7), for the cable–damper system with $l_1/L = 0.02$, $\lambda = 0.01$(s), $\omega_{o1} = 4.152$ (rad/s). Fig. 3(b) depicts the exact solutions. It turns out that the attainable modal damping ratios obtained by Eq. (7) are only slightly smaller than the exact solutions. However, both the asymptotic solutions and exact solutions show that the attainable modal damping ratios are smaller for higher mode of vibration. This is due to the relaxation time constant, which is different from the case of the cable with a linear viscous damper where the relaxation time constant is zero and all the curves overlap with each other. The effects of relaxation time constant on attainable modal damping ratio can be found in Fig. 4 for $\lambda = 0.01$, 0.04, 0.06(s) and for $l_1/L = 0.02$, $i = 1$, $\omega_{o1} = 4.152$ (rad/s), in which the results in Fig. 4(a) are obtained from the asymptotic solution while those in Fig. 4(b) are computed using the exact solution. The use of λ rather than the nondimensional quantity $\lambda\omega_{o1}$ is to be consistent with the experimental results provided in Ref. [11]. Again, the asymptotic results are very close to the accurate results for different relaxation time constants λ. The maximum attainable nondimensional modal damping ratio decreases as the relaxation time constant λ increases; such a reduction accounts for about 20% when the relaxation time constant $\lambda = 0.06$ (s) comparing to $\lambda = 0$. As the relaxation time constant is associated with the damper stiffness and the damper support stiffness, one may conclude that both the damper stiffness and the damper support stiffness will reduce the control effectiveness of the damper. Thus, it may be necessary to include the frequency dependence property in the analysis if a damper exhibits Maxwell characteristics and/or the damper support is not stiff enough.

4. Most favorable design principles

From Eqs. (7) and (8), one may find that when a fluid damper is installed at a given location of a cable, the damper will have an optimum viscous coefficient of the damper that can achieve the maximum modal damping ratio in the cable. The optimum viscous coefficient of the damper, however, depends on not only

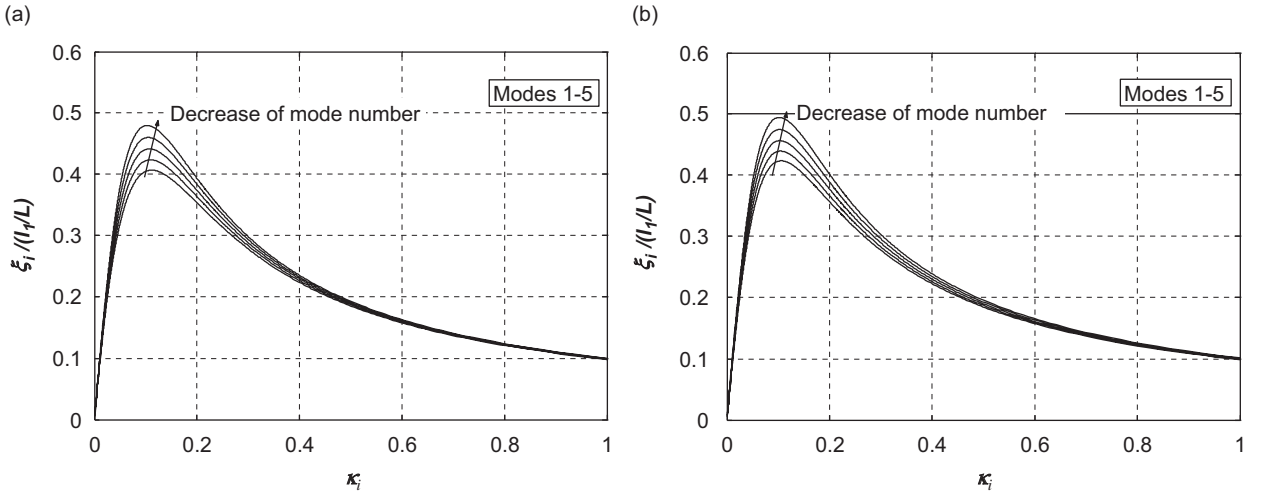

Fig. 3. Cable modal damping ratio vs. nondimensional viscous coefficient of the damper ($l_1/L = 0.02$, $\lambda = 0.01$ (s), $\omega_{o1} = 4.152\,(s^{-1})$, $i = 1-5$): (a) asymptotic solutions, and (b) exact solutions.

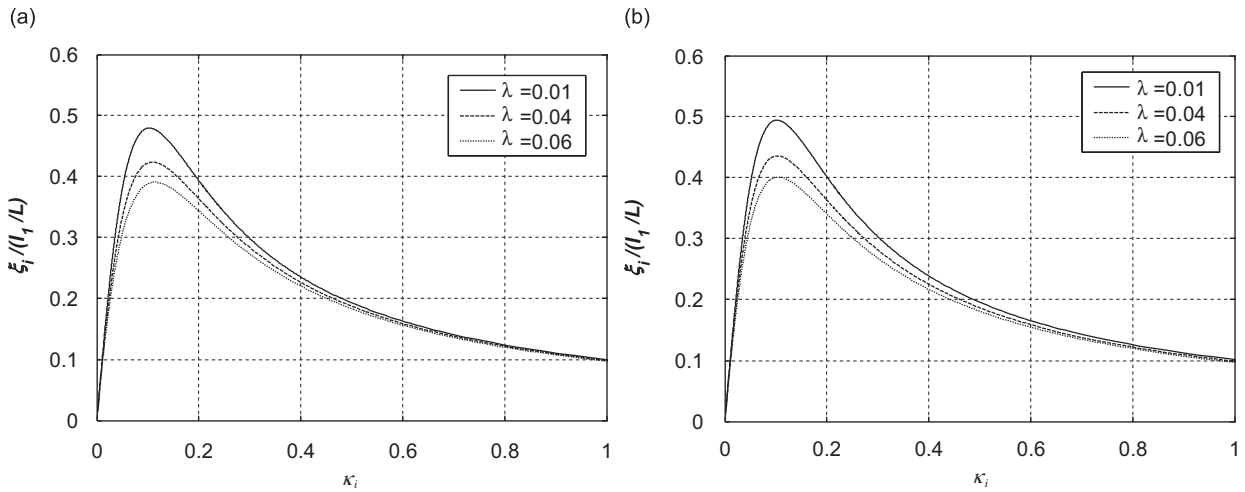

Fig. 4. Effects of relaxation time constant ($l_1/L = 0.02$, $\lambda = 0.01-0.06$ (s), $\omega_{o1} = 4.152\,(s^{-1})$, $i = 1$): (a) asymptotic solutions, and (b) exact solutions.

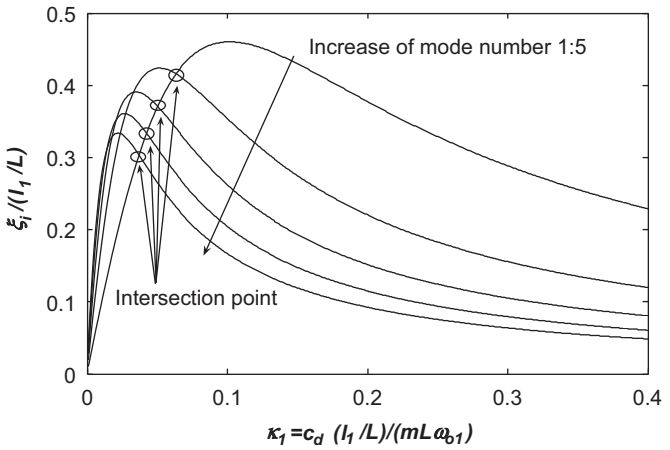

Fig. 5. Intersection points for nondimensional viscous coefficient of the damper ($l_1/L = 0.02$, $\lambda = 0.02$(s), $\omega_{o1} = 4.152(s^{-1})$, $i = 1{:}5$).

cable properties but also cable vibration mode. Let us consider a cable–damper system with $l_1/L = 0.02$, $\lambda = 0.02$(s), $\omega_{o1} = 4.152$ (rad/s). Fig. 5 plots the normalized modal damping ratios against the first nondimensional viscous coefficient of the damper $\kappa_1 = c_d(l_1/L)/(mL\omega_{o1})$ for the first five modes of vibration based on Eq. (7). It can be seen that the lower mode of vibration has the higher maximum modal damping ratio. The corresponding optimum viscous coefficient of the damper c_d is also significantly different from each other; the lower mode of vibration needs the larger optimum viscous coefficient of the damper. Clearly, it is not possible for one fluid damper to achieve the maximum modal damping ratio for all modes of vibration of a given cable. Furthermore, as optimum viscous coefficient of the damper depends on the properties and vibration modes of the cable and the location of the damper, it will be different for different cables. This implies that every cable needs its own damper ideally. However, this will cause many problems in the process of manufacture, installation and maintenance. Therefore, some compromise must be made and the grouping process is unavoidable in practice. This study proposes a most favorable design principle to select the favorable viscous coefficient of the damper for each cable and group these favorable viscous coefficients of the damper according to the adjustable levels of one or two adjustable fluid dampers.

The most favorable design principle is to select the number of modes of vibration required to be damped for all stay cables in a cable-stayed bridge and at the same time to comply with the requirement that the modal

damping ratios in the concerned vibration modes for all stay cables should be greater than the least modal damping ratio limit ζ_{limit}. The determination of the least modal damping ratio ζ_{limit} should consider many practical factors. For instance, it may be selected as 0.5% damping ratio or 3% logarithmic decrement [13]. By adopting this favorable design principle, one should plot the ζ_i–c_d curves similar to those in Fig. 5 for each cable. Then, select the initial number of modes of vibration required to be damped, for instance i. Find the intersection point of the ith modal damping ratio curve and the first modal damping ratio curve for each cable from their ζ_i–c_d curves. The viscous coefficient of the damper corresponding to the intersection point can then be regarded as the favorable viscous coefficient of the damper and the corresponding modal damping ratio is regarded as the favorable modal damping ratio. If not all the favorable modal damping ratios are greater than ζ_{limit}, the number of modes of vibration required to be damped should be reduced until all the favorable modal damping ratios are greater than ζ_{limit}. The favorable viscous coefficient of the damper for each cable can be found using Eq. (7). Let

$$\frac{\zeta_1}{l_1/L}=\frac{\zeta_i}{l_1/L}\Rightarrow\frac{\pi^2\frac{c_d}{mL\omega_{o1}}(l_1/L)}{1+\left[\pi^2\frac{c_d}{mL\omega_{o1}}(l_1/L)+\lambda\omega_{o1}\right]^2}=\frac{\pi^2\frac{c_d}{mL\omega_{o1}}\mathrm{i}(l_1/L)}{1+\left[\pi^2\frac{c_d}{mL\omega_{o1}}\mathrm{i}(l_1/L)+\mathrm{i}\lambda\omega_{o1}\right]^2} \tag{9}$$

then

$$c_{d,\text{opt}}=\frac{mL\omega_{o1}}{\pi^2(l_1/L)}\left(\frac{1}{\sqrt{\mathrm{i}}}-\lambda\omega_{o1}\right), \tag{10}$$

where $c_{d,\ \text{opt}}$ is the favorable viscous coefficient of the damper.

5. Case study

5.1. A long span cable-stayed bridge

The long span cable-stayed bridge taken as a case study has a total length of 1596 m and a main span of 1018 m. The height of the two towers is nearly 300 m, measured from the base level to the top of towers. The bridge tower is of single composite column, and the stay cables are of the parallel wire strand type made up of 7 mm wires. There are a total of 224 stay cables, and the length of the longest stay cable is about 540 m.

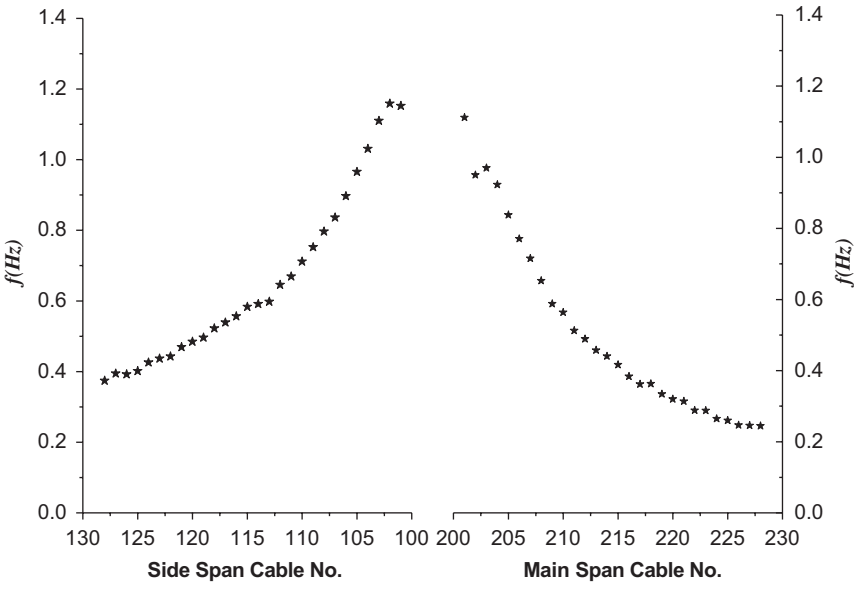

Fig. 6. First natural frequencies of stay cables.

For the sake of clear presentation, only one quarter of stay cables of the bridge are considered, including 28 stay cables in the main span and 28 stay cables in the side span. Fig. 6 displays the computed first natural frequency, $f_1 = \omega_{o1}/(2\pi)$, of each cable without any damper. The lowest first natural frequency is 0.244 Hz for the cable No. 228 in the main span and the highest first natural frequency is 1.159 Hz for the cable No. 102 in the side span. Fig. 7 shows the ratio of the damper location to the original cable length, l_1/L, for each cable. The ratio ranges from 0.018 to 0.031. Let us assume that only one adjustable fluid damper is installed perpendicularly to the cable axis in the vertical plane near the low cable anchorage for each cable. As discussed before, the effect of the damper support stiffness may be considered. Fig. 8 displays the damper support stiffness for each cable. It can be seen that the damper support stiffness has an increasing tendency as cable length becomes shorter.

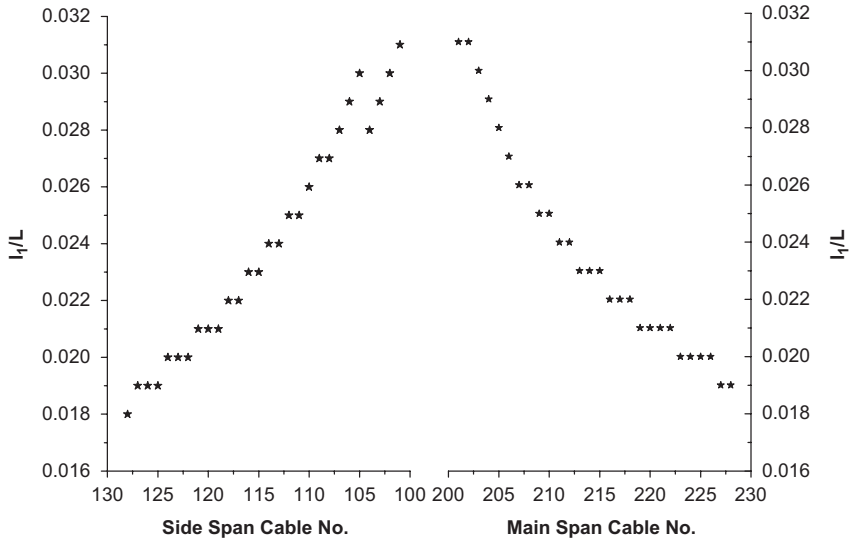

Fig. 7. Ratios of damper location to cable length.

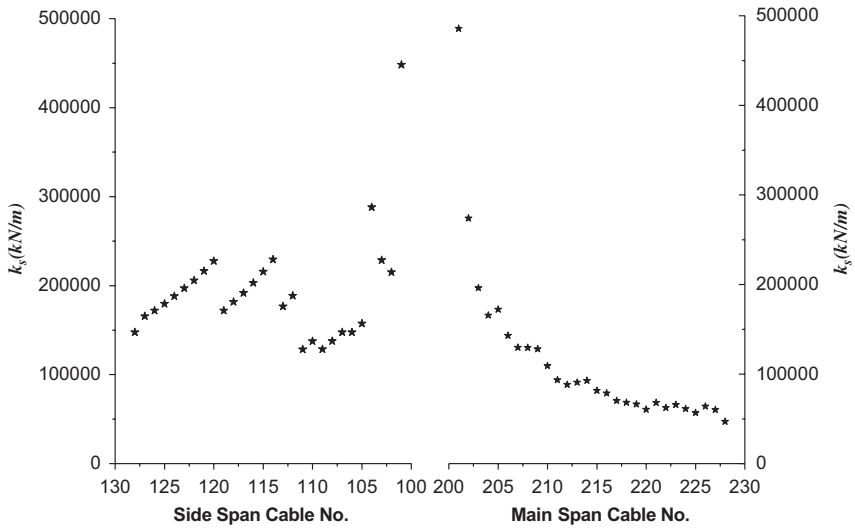

Fig. 8. Damper support stiffness for each cable.

5.2. Favorable design of adjustable fluid dampers

The favorable design principle is used in this case study and the number of vibration modes is taken as two for all the stay cables concerned. The favorable design of adjustable fluid dampers is, in fact, an iterative process.

Firstly, assume the damper is an ideally linear viscous damper and the damper support is perfectly rigid so that the relaxation time constant is equal to zero. Then, use Eq. (10) to find the initial favorable viscous coefficient of the damper for each cable, as shown in Fig. 9 for stay cables in the side span and in Fig. 10 for stay cables in the main span. Based on such information, adjustable fluid dampers are designed with enough adjustable levels covering a wide range of viscous coefficient of the damper. The adjustable fluid dampers are manufactured and calibrated to find their viscous coefficient of the damper and relaxation time constants. In this case study, two types of prototype adjustable fluid dampers, which have ten orifices in the piston head and eight of them controllable for achieving changes in damping at 9 levels, were designed and manufactured: type 1 with 1.5 mm diameter orifices for large viscous coefficient of the damper; and type 2 with 1.8 mm diameter orifices for relatively small viscous coefficient of the damper. The two prototype dampers were extensively calibrated and tested. The viscous coefficient of the damper and the relaxation time constants obtained from the tests are listed in Table 1. According to the viscous coefficient of the damper available in Table 1 and the required initial favorable viscous coefficient of the damper shown in Figs. 9 and 10, one may decide that the damper type 2 is used for those cables requiring a favorable viscous coefficient of the damper below 173,000 N s/m and the damper type 1 is used for all other cables. One may also decide the adjustable levels of each damper using the number of opened orifices in the damper to best fit the initial favorable viscous coefficient of the damper. Fig. 11 shows the grouping results of damper type and adjustable level. The next step is to calculate the total relaxation time constant for each cable, which includes both damper stiffness and damper support stiffness, as shown in Fig. 12. The results shown in Fig. 12 indicate that in this case study, the damper support stiffness is much larger than the damper stiffness. Eq. (10) is then used again to determine the favorable viscous coefficient of the damper but with the relaxation time constants included. These results are plotted in Figs. 9 and 10 and compared with the grouping results. If the comparison is not satisfactory, the grouping can be finely tuned until both are close to each other. One may see from Figs. 9 and 10 that some differences exist between the initial and final favorable viscous coefficient of the damper but they

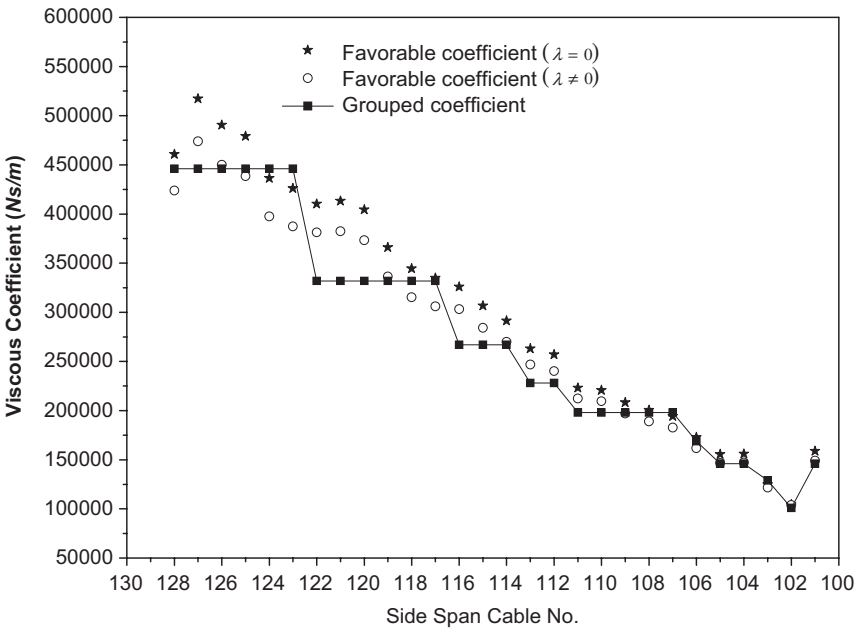

Fig. 9. Viscous coefficient of the damper for stay cables in side span.

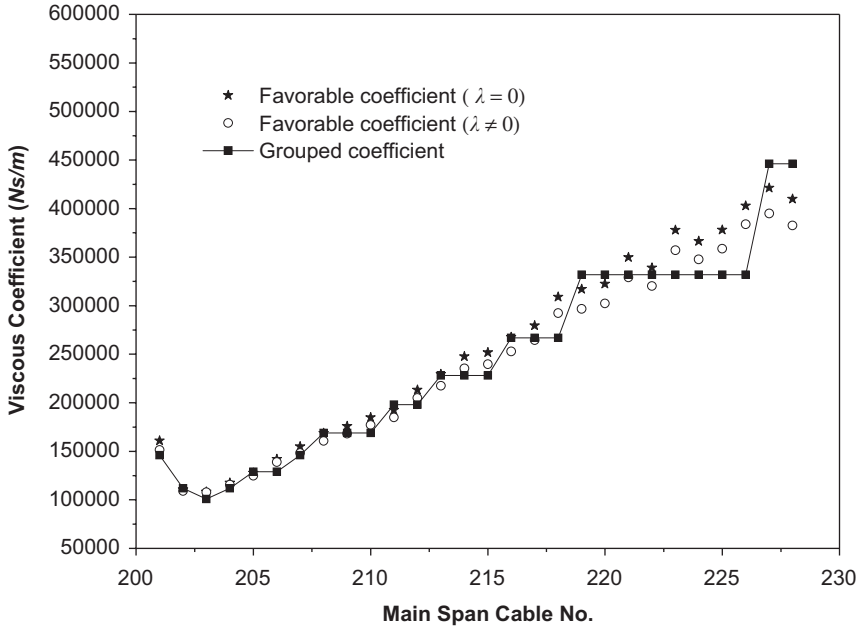

Fig. 10. Viscous coefficient of the damper for stay cables in main span.

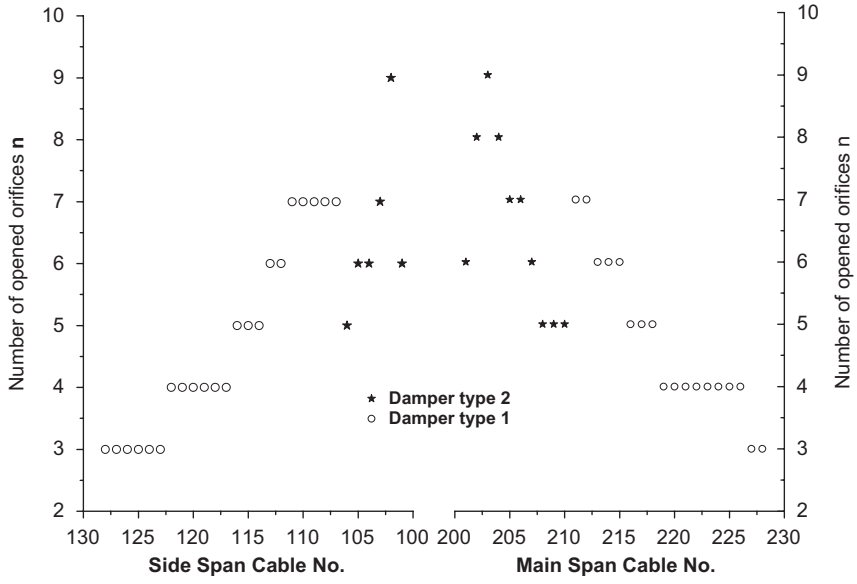

Fig. 11. Grouping results of damper type and adjustable level.

are not very significant because only the first two modes of vibration are considered in this case study. Finally, based on the final grouping results, one may re-calculate the favorable modal damping ratios in the first two modes of vibration for each cable and check if they are greater than ζ_{limit}. The favorable modal damping logarithmic decrements obtained and shown in Fig. 13 for this case study demonstrate that the modal damping logarithmic decrements in the first two modes of all the stay cables concerned are greater than 4%. It should be pointed out, however, that the favorable modal damping logarithmic decrements shown in Fig. 13 are obtained based on the assumption of a taut cable. For the first mode of vibration of the longest stay cable, sag effect may reduce the modal damping logarithmic decrement to some extent.

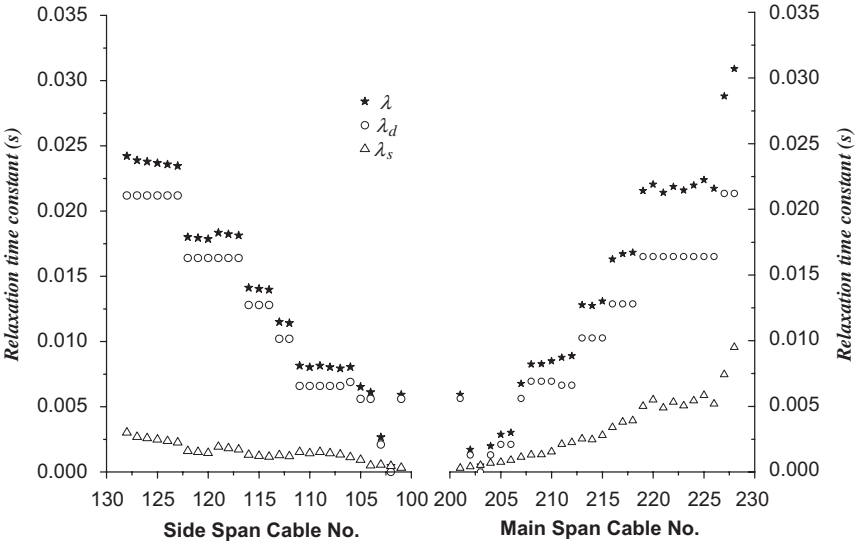

Fig. 12. Relaxation time constants λ, λ_d, λ_s.

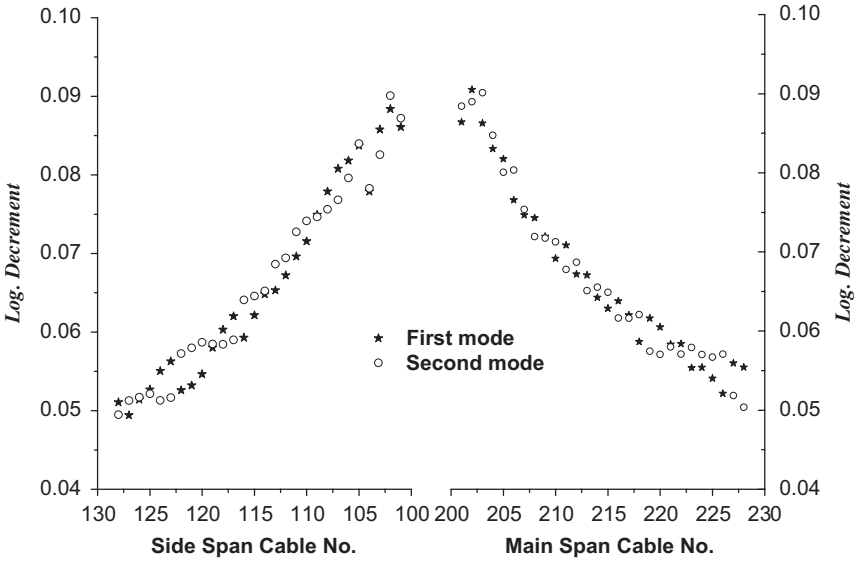

Fig. 13. Modal damping logarithmic decrements in stay cables.

6. Conclusions

The adjustable fluid dampers with shape memory alloy actuators, which can be well described by the Maxwell model, have been introduced in this paper. The asymptotic solutions have been found to determine the optimum viscous coefficient of the damper of an adjustable fluid damper. The most favorable design procedure with a grouping process has been proposed for selecting the least types of adjustable fluid dampers to damp vibration of a few hundreds stay cables and has been applied to stay cables in a super long span cable-stayed bridge as a case study. The results from the case study demonstrate that only two types of adjustable fluid dampers are required for damping vibration of all stay cables in the bridge. The modal damping

logarithmic decrements in the first two modes of all the stay cables all are greater than 4% even considering the effects of damper stiffness and damper support stiffness. It should be pointed out that the proposed approach is valid for a taut cable and for damper location very close to cable anchorage.

Acknowledgements

The work described in this paper was financially supported by the Research Grants Council of Hong Kong (Project No. PolyU1/02C), to which the writers are grateful.

References

[1] Y. Hikami, N. Shiraishi, Rain-wind induced vibration of cables in cable stayed bridges, *Journal of Wind Engineering and Industrial Aerodynamics* 29 (1988) 409–418.
[2] J.A. Main, N.P. Jones, Evaluation of viscous dampers for stay-cable vibration mitigation, *Journal of Bridge Engineering ASCE* 6 (6) (2001) 385–397.
[3] H. Yamaguchi, Y. Fujino, Stayed cable dynamics and its vibration control, in: A. Larsen, S. Esdahl (Eds.), *Proceedings of the International Symposium on Advances in Bridge Aerodynamics*, A.A. Balkema, Rotterdam, 1998, pp. 235–253.
[4] B.M. Pacheco, Y. Fujino, A. Sulekh, Estimation curve for modal damping in stay cables with viscous damper, *Journal of Structural Engineering ASCE* 119 (6) (1993) 1961–1979.
[5] S. Krenk, Vibration of a taut cable with an external damper, *Journal of Applied Mechanics ASME* 67 (2000) 772–776.
[6] J.A. Main, N.P. Jones, Free vibrations of cable with attached damper. Part I: linear viscous damper, *Journal of Engineering Mechanics ASCE* 128 (2002) 1062–1071.
[7] S. Krenk, J.R. Høgsberg, Damping of cables by a transverse force, *Journal of Engineering Mechanics ASCE* 131 (4) (2005) 340–348.
[8] Z. Yu, Y.L. Xu, Mitigation of three-dimensional vibration of inclined sag cable using discrete oil damper. Part I: formulation, *Journal of Sound and Vibration* 214 (4) (1998) 659–673.
[9] Y.L. Xu, Z. Yu, Mitigation of three-dimensional vibration of inclined sag cable using discrete oil damper. Part II: application, *Journal of Sound and Vibration* 214 (4) (1998) 674–693.
[10] R.E. Christenson, B.F. Spencer, E.A. Johnson, Experimental verification of smart cable damping, *Journal of Engineering Mechanics ASCE* 132 (3) (2006) 268–278.
[11] Z.Q. Li, Y.L. Xu, L.M. Zhou, Adjustable fluid damper with SMA actuators, *Smart Materials & Structures* 15 (5) (2006) 1483–1492.
[12] M.P. Singh, N.P. Verma, L.M. Moreschi, Seismic analysis and design with Maxwell dampers, *Journal of Engineering Mechanics ASCE* 129 (3) (2003) 273–282.
[13] J.A. Main, Modeling the Vibrations of a Stay Cable with Attached Damper, PhD Thesis, The Johns Hopkins University, 2002.